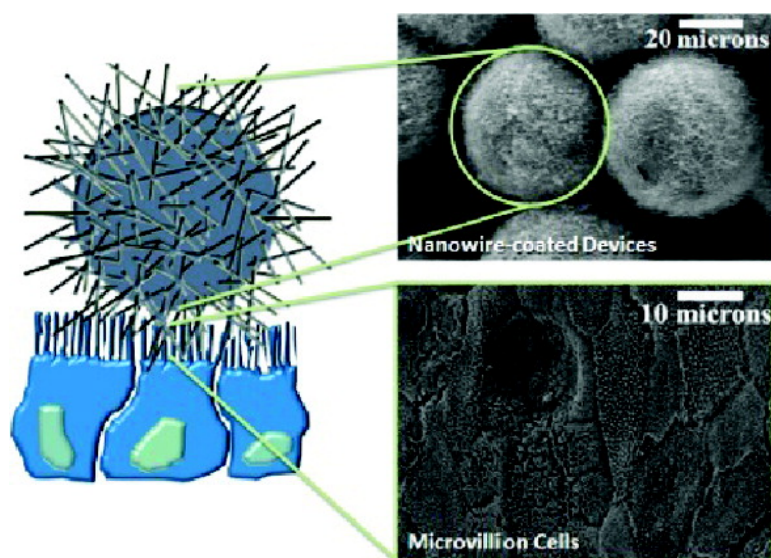


Biomimetic Nanowire Coatings for Next Generation Adhesive Drug Delivery Systems

Kathleen E. Fischer, Benjamin J. Aleman, Sarah L. Tao, R. Hugh Daniels, Esther M. Li, Mark D. Buehner, Ganesh Nagaraj, Parminder Singh, Alex Zettl, and Tejal A. Desai

Nano Lett., 2009, 9 (2), 716-720 • DOI: 10.1021/nl803219f • Publication Date (Web): 21 January 2009

Downloaded from <http://pubs.acs.org> on February 17, 2009



More About This Article

Additional resources and features associated with this article are available within the HTML version:

- Supporting Information
- Access to high resolution figures
- Links to articles and content related to this article
- Copyright permission to reproduce figures and/or text from this article

[View the Full Text HTML](#)

Biomimetic Nanowire Coatings for Next Generation Adhesive Drug Delivery Systems

Kathleen E. Fischer,^{†,‡,§,+} Benjamin J. Alemán,^{||,⊥,#,+} Sarah L. Tao,^{∇,+}
R. Hugh Daniels,^{||,+} Esther M. Li,^{||,+} Mark D. Büngrer,^{†,‡,+} Ganesh Nagaraj,^{†,‡,+}
Parminder Singh,^{†,‡,+} Alex Zettl,^{||,⊥,#,+} and Tejal A. Desai^{*,†,‡,§}

Department of Bioengineering and Therapeutic Sciences, Department of Physiology, University of California, San Francisco, San Francisco, California 94158, UCSF/UCB Joint Graduate Group in Bioengineering, San Francisco, California 94158, Material Science Division of LBNL, Berkeley, California 94720, Center of Integrated Nanomechanical Systems (COINS), Berkeley, California 94720, Department of Physics, University of California, Berkeley, Berkeley, California 94720, The Charles Stark Draper Laboratory, Cambridge, Massachusetts 02139, and Nanosys, Inc., Palo Alto, California 94304

Received October 23, 2008; Revised Manuscript Received December 16, 2008

ABSTRACT

Without bioadhesive delivery devices, complex compounds are typically degraded or cleared from mucosal tissues by the mucous layer.^{1–3} While some chemically modified, microstructured surfaces have been studied in aqueous environments,^{4,5} adhesion due to geometry alone has not been investigated. Silicon nanowire-coated beads show significantly better adhesion than those with targeting agents under shear, and can increase the lift-off force 100-fold. We have shown that nanowire coatings, paired with epithelial physiology, significantly increase adhesion in mucosal conditions.

Because of their easy accessibility, large surface area, and rich blood supply, mucous membranes (mucosae), such as intestinal, nasal, ocular, vaginal, and buccal tissues, are frequently targeted for therapeutic drug delivery.^{1,6} However, the mucosae present significant barriers to permeation, including a 1–450 μm motile mucous gel layer, tight junctions, and in some tissues, harsh enzymes and low pH.⁷ Delivery devices have been able to protect compounds from chemical degradation, but without adhesion to the underlying epithelium, the devices are cleared with the lumen contents or with the mucous layer in a matter of hours.^{1–3,8} A short

transit time in conjunction with chemical degradation produce a relatively low concentration gradient at the cellular surface and thus reduced compound absorption. Specific epithelial targeting agents, such as lectins, adhere to glycosaminoglycans on the cell surface; because these sugars are found in the mucous layer as well, competition between the mucous layer and cell surface for binding to mucoadhesives reduces the amount of direct device-cell binding to that of nonadhesive controls, particularly in vivo.^{9,10} Furthermore, mucoadhesives are constrained by the mucin turnover time (50–170 min¹¹), whereas devices that directly bind to cells are only constrained by the cell turnover time (2–3 days¹²). Thus, for robust mucosal adhesion, a device must penetrate the mucous layer and adhere directly to the epithelium.

One particularly promising class of adhesives is gecko-inspired (geometry-based) adhesives. Micro- and nanostructured surfaces naturally occur in a variety of insects and lizards and have been shown to rely primarily on van der Waals forces for adhesion.^{13–18} While numerous experiments have shown biomimetic nanowires and nanotubes to adhere with forces ranging from 0.04^{19,20} to 30 times²¹ the adhesive strength of geckos (reported to be 500 kPa¹⁶) in dry environments,^{22,23} only two groups have looked at submicron

* To whom correspondence should be addressed. E-mail: Tejal.Desai@ucsf.edu. Phone: 415-514-4503. Fax: 415-476-2414.

[†] Department of Bioengineering and Therapeutic Sciences, University of California, San Francisco.

[‡] Department of Physiology, University of California, San Francisco.

[§] UCSF/UCB Joint Graduate Group in Bioengineering.

^{||} Material Science Division of LBNL.

[⊥] Center of Integrated Nanomechanical Systems (COINS).

[#] Department of Physics, University of California, Berkeley.

[∇] The Charles Stark Draper Laboratory.

⁺ Nanosys, Inc.

⁺ Additional e-mail addresses: (K.E.F.) kayte@berkeley.edu; (B.J.A.) benji@berkeley.edu; (S.L.T.) stao@draper.com; (R.H.D.) HDaniels@nanosysinc.com; (E.M.L.) ELi@nanosysinc.com (M.D.B.) mark.bunger@luxresearchinc.com (G.N.) gnagaraj87@gmail.com; (P.S.) parmindsingh@gmail.com; (A.Z.) azettl@physics.berkeley.edu.

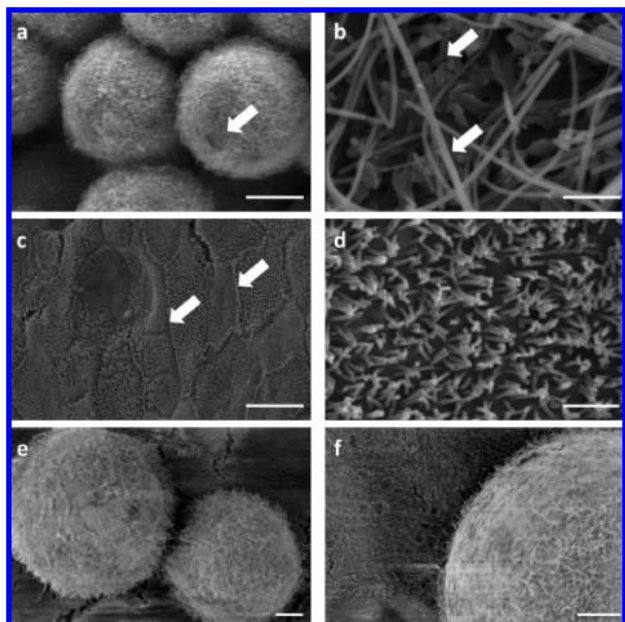


Figure 1. Nanowire–cell interactions. (a) Scanning electron micrograph showing nanowire-coated microspheres with extensive nanowire coating. Arrow indicates an area of reduced nanowire coverage. Scale bar is 20 μm . (b) Intestinal microvilli (top arrow) interdigitate with matted nanowires on the apical surface of the cells (bottom arrow). Scale bar is 500 nm. (c) Caco-2 cells form a monolayer. Individual cells can be identified by their borders (arrows). Scale bar is 10 μm . (d) Intestinal microvilli have nanoscale diameters, averaging 71.8 ± 10.5 nm. Scale bar is 1 μm . (e) Two nanowire-coated microspheres sit on top of cells. Scale bar is 10 μm . (f) Nanowires on the side of a microsphere interacting with microvilli on cells. Scale bar is 5 μm .

structures in aqueous conditions (elements of diameter 0.4 μm for Lee et al.⁵ and 0.1–1 μm for Mahdavi et al.⁴). Despite using microstructured surfaces, in a wet environment chemical modification was necessary to bolster adhesion.

Under nanoadhesive conditions, as the number of adhesive elements per surface area increases (i.e., diameter of individual elements decreases), the surface area to volume ratio increases and van der Waals adhesion is predicted to increase.^{24,25} Furthermore, because mucosal epithelia exhibit nanostructured microvilli, available surface area contact is considerably increased on the cell surface.^{26–29} Thus, by decreasing the diameter of the elements on the device surface to the nanoscale and targeting a microvilliated surface, it may be possible to generate strong bioadhesive forces due to geometric features alone.

To test the interaction of microvilli and nanostructures, a prototype device was created to couple the adhesive characteristics of nanowires with the drug delivery capacity of beads. A standard vapor–liquid–solid method for synthesizing silicon nanowires on flat wafer surfaces was modified to achieve growth of size-specific nanowires on the surface of 30–50 μm diameter glass beads (Figure 1).³⁰

A Caco-2 cell monolayer was used as an in vitro model of the intestinal mucosa because the cells display a microvilliated structure which closely corresponds to that found in vivo.³¹ From scanning electron microscopy (Figure 1b), significant interdigitation of the nanowires and microvilli was

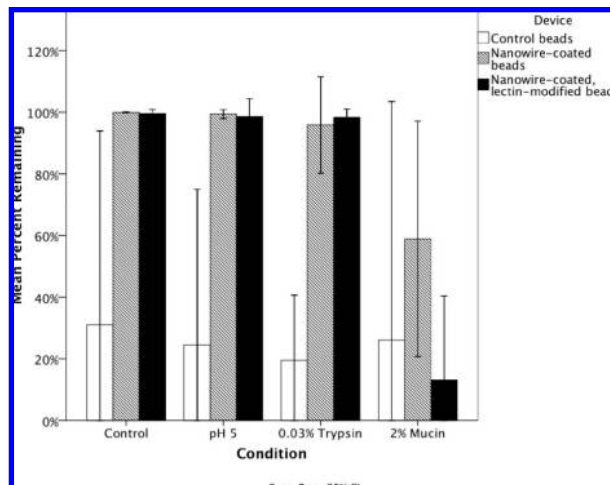


Figure 2. Static Adhesion. Percent adhesion after incubation on cells in different solutions and subsequent washes with media. HBSS was used as a control. Two-way ANOVA shows significance in comparisons of the conditions, the devices, and between the conditions and devices. To compare data in the plot, error bars represent 95% confidence intervals. Multiple comparisons between the devices using a Bonferroni correction indicate significant differences between the control beads and the nanowire-coated beads ($p < 0.05$) and between the control beads and the nanowire-coated, lectin-modified beads ($p < 0.05$). Multiple comparisons between the conditions using a Bonferroni correction indicate a significant difference between 2% Mucin and all other conditions.

visible at the cell–nanostructure interface, showing significant areas of contact between the cells and nanowires.

In order to characterize the effects of geometric and chemical modifications of the nanowires, three nanowire test geometries and a control group with no nanowires (See Table 1 in Supporting Information) were fabricated. A subset of the long nanowire group and the control group were chemically modified with tomato lectin, a well-characterized mucoadhesive intestinal targeting molecule.^{10,32,33} Each test geometry had nanowires with an average diameter of 60 nanometers, but with varying lengths and numbers of adhesive elements per surface area (coating densities). Within each geometry, the quality of surface area nanowire coverage varied bead by bead (expressed as percent surface area covered).

To isolate the effects of various factors within the mucosal environment that could lead to reduced adhesion, devices were incubated with cells while in the presence of either Hanks balanced salt solution (HBSS), 2% w/v mucin, HBSS at $\text{pH } 5.1 \pm 1.0$ (s.d.), or 0.03% trypsin (Figure 2). In all solutions, nanowire-coated beads adhered to cells at a frequency 5 times greater than control beads. Additionally, except in the mucin solution, the tomato lectin-modified, nanowire-coated devices adhered as well or slightly better than the nanowire-coated beads, indicating that these solutions have no significant effect on the targeting capabilities of tomato lectin.³⁴ The reduced adhesion of lectin modified, nanowire-coated devices in mucin suggests that unmodified nanowire-coated devices may have an advantage when exposed to mucus.

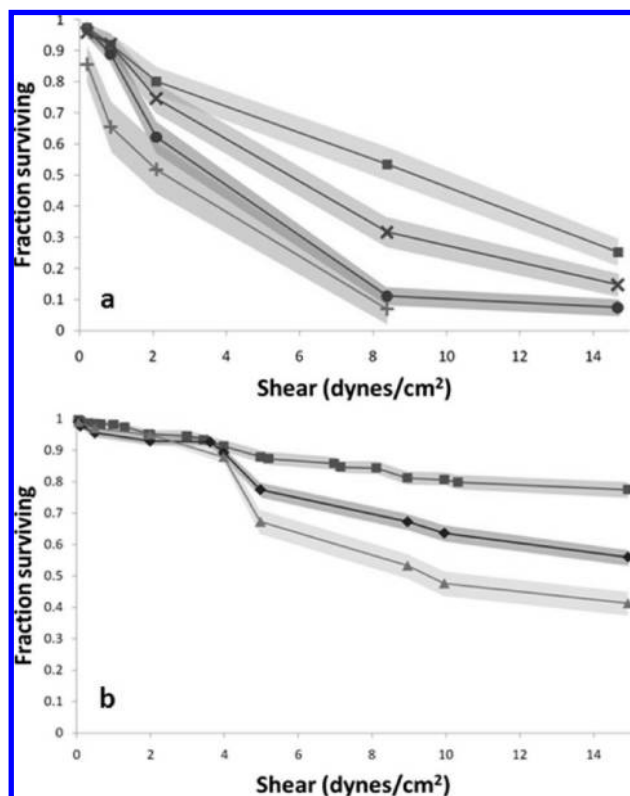


Figure 3. Device survival rates under shear flow with 95% confidence intervals shown in the respective shaded areas. (a) Modified and unmodified device survival in 2% mucin flow (■, nanowires; ×, lectin-modified, nanowire-coated devices; ●, lectin-modified devices; +, control devices). The unmodified control beads survive at a significantly lower rate ($n = 4$, $p < 0.05$, as indicated by distinct 95% confidence intervals calculated using a Kaplan–Meier survival curve) than the nanowire coated beads for all shears, whereas the lectin modified beads and lectin-modified, nanowire-coated beads significantly differ from nanowire-coated beads above shears of 1.5 and 3.5 dynes/cm², respectively. (b) Survival of devices with varying nanowire geometry in media (■, long nanowires; ◆, medium nanowires; ▲, short nanowires). In this experiment, $n = 6$.

Lectin-modified and unmodified devices incubated on a Caco-2 monolayer were exposed to mucin flow to determine the effect of chemical modification on adhesion under shear stress (Figure 3a). Unmodified control beads and lectin-modified beads detached at the lowest shears with median survival shears, the shear at which 50% of the devices had detached, of 2.35 and 3.60 dynes/cm², respectively. Though lectin-modified nanowires decreased the level of bead detachment, unmodified nanowires showed the greatest retention (median survival shears of 5.70 and 9.15 dynes/cm², respectively). Compared to unmodified nanowires, lectin modification enhanced detachment from cells under mucous flow, indicating that mucoadhesive chemistry may reduce overall mucosal tissue adhesion, compared to geometry-based adhesion. Because lectins bind to both cells and mucus, adding a mucin layer introduces competition between these elements for binding to the lectin-modified nanowires, which may explain the reduced adhesion.

Shear flow studies conducted on nanowires with varying geometric properties indicated strong device retention rates,

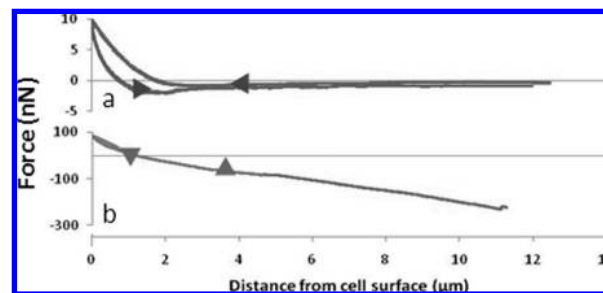


Figure 4. Typical AFM adhesion force curves. (a) Control beads with no nanowires show adhesive forces around 0.5–2 nN. (b) Nanowire-coated beads with good coating show maximal adhesive forces upward of 100 nN and can exhibit forces upward of 100 times greater than control beads.

above 90%, for all geometries in shear less than 4 dynes/cm² with the long nanowires providing the greatest adhesion at higher shears (median survival shear of 54.40 dynes/cm²). The median survival shears for the medium and short nanowires were 17.79 and 9.54 dynes/cm², respectively. The median survival shear correlated to the length of nanowires, indicating a relationship between nanowire length and adhesion under shear flow.

An atomic force microscope (AFM) with devices affixed to cantilevers was used to quantitatively determine tensile adhesive forces. Typical curves from this system (Figure 4) indicated that control beads produced an adhesion force of 1.80 ± 0.2 nN (sem) when contacting cells. When a nanowire-coated bead made contact with cells, forces upward of 100 nN were common (mean force: 172.0 ± 53.8 nN sem). In some cases, it was possible to visualize the apparent adhesion of single nanowires or small clusters of nanowires (see Supporting Information).

Using scanning electron microscopy after AFM experiments, length and surface area coverage of a given bead were quantified to determine the relationship between nanowire geometry and maximal forces generated in the AFM experiments (Figure 5). At one extreme, short nanowires provided a smaller increase in surface area than longer nanowires, reducing available contact forces comparatively; at another extreme, long nanowires tended to fold over on themselves, creating a matted surface and reducing the overall available surface area compared to freestanding nanowires. Accordingly, within our AFM testing length range (0–3 μm nanowire length), the data suggest that it is possible to optimize adhesion by growing nanowires between 1 and 2 μm (Figure 5a). In addition to nanowire length, the quality of surface area coverage affected maximum forces achieved with devices exhibiting reduced coverage, such as those that contain patches without nanowires, achieving lower maximum forces (Figure 5b). On the basis of surface area coverage and maximum force measurements, the force of adhesion of nanowire-coated devices was found to be 0.11 kPa; this estimation is a lower limit (see Supporting Information).

In addition to nanowire geometry and chemistry, we considered physiologically relevant variations in the geometry and chemistry of the underlying cell surface. Because

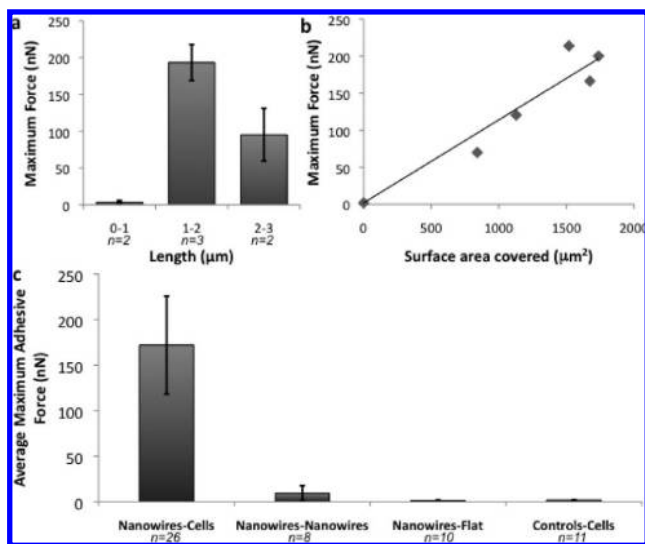


Figure 5. Geometric effects on maximum force. (a) Maximum force varies over a range of nanowire lengths indicating an optimal length of 1–2 μm in the range investigated. (b) Maximum force increases linearly with surface area coverage; linear regression yields $r^2 = 0.91$. On the basis of this regression, the maximum adhesive force is calculated to be 0.11 kPa. (c) Average maximum adhesive forces varying by device-substrate pairings. The nanowire-cells pairing is significantly different from the nanowire-flat and control beads-cells pairings. Otherwise, differences are not significant. Error bars indicate standard error of the mean.

much of the documented dry nanostructure adhesion is due to van der Waals forces, which are dependent on the surface area in contact with the substrate, a nanostructured surface (such as a cell with microvilli or a nanowire-coated bead) would be expected to increase the adhesion over a flat surface. As expected, nanowire-coated beads brought into contact with flat polystyrene produced a mean force of adhesion of 1.30 ± 0.5 nN (sem); however, a nanowire-coated bead in contact with a nanowire substrate only increased the adhesion force to 9.3 ± 8.4 nN, still an order of magnitude less than the mean adhesion between nanowires and cells (Figure 5c). This minor increase suggests that forces beyond van der Waals forces may be responsible for a significant proportion of nanowire-cell adhesion.

In this paper, nanowires were shown to significantly increase bead adhesion compared to uncoated control beads. Furthermore, devices with a nanowire coating adhered to cells as well as chemically targeted devices in common in vitro conditions and better than chemically targeted devices when exposed to relevant physiological conditions such as a mucous layer and shear flow. Varying the length and surface area coverage of the nanowires further optimized adhesion. Mimicking the nanoscale microvilli with a nanowire surface (nanowire–nanowire adhesion) did not yield equivalent force to cell–nanowire adhesion, indicating that forces beyond van der Waals forces may be at work. While nanowires cannot move appreciably after contact, microvilli could rearrange themselves, creating more intimate contact, increasing surface area related forces, and possibly altering their shape to produce physical adhesion, similar to the interlocking interaction of Velcro.

Furthermore, because nanowire-coated devices have non-specific adhesive interactions, they may also adhere to other gastrointestinal cells, such as those in the esophagus or stomach. To bypass these undesired regions, the devices may be encapsulated in an enteric capsule that only dissolves in the intestinal pH range.

Though a few nanoparticle delivery systems have been found to be immunogenic in certain situations,³⁵ silicon nanowire-coated surfaces have been shown to elicit a less immunogenic response than that of bulk silicon.³⁶ Additionally, because the nanowires are physically attached to the surface of a microsphere, they are unlikely to be ingested by cells, and thus unlikely to collect in other organs, such as the liver or spleen.

Nanowire-based, inorganic bioadhesives are attractive for mucosal drug delivery systems because they reduce interactions with therapeutic compounds and are robust even in degrading environments, such as the gastrointestinal system. Silicon is particularly interesting for biological applications because it is slowly degraded compared to mucosal turnover rates in vivo, has a variety of well-characterized nanowire fabrication techniques, and could be integrated into other silicon-based systems, such as microelectromechanical systems (MEMS) sensors or other smart systems.^{37,38} Furthermore, nanostructured adhesive surfaces may be useful in numerous clinical applications, such as soft tissue adhesives and engineered tissue implants.

Acknowledgment. Funding support was from Nanosys, Inc., the University of California Discovery Grant, the National Institutes of Health under Grant R01 EB002687, the Sandler Family Foundation, and the Rogers Foundation. This work was also supported by the National Science Foundation within the Center of Integrated Nanomechanical Systems, under Grant EEC-0425941, and by the Director, Office of Energy Research, Office of Basic Energy Sciences, Materials Sciences and Engineering Division, of the U.S. Department of Energy under contract DE-AC02-05CH11231 that provided for sample characterization. A portion of the scanning electron microscopy was done at the Stanford Nanocharacterization Laboratory through the Center for Integrated Systems grant program. K.F. wishes to acknowledge graduate funding from the NSF GRFP award and help with manuscript preparation from Kristy M. Ainslie and Dan A. Bernards.

Supporting Information Available: Further descriptions of the methods used in this paper, as well as an interpretation of the atomic force microscopy results in the context of these experiments. This material is available free of charge via the Internet at <http://pubs.acs.org>.

References

- (1) Lee, J. W.; Park, J. H.; Robinson, J. R. Bioadhesive-based dosage forms: The next generation. *J. Pharm. Sci.* **2000**, *89*, 850–866.
- (2) Norris, D. A.; Puri, N.; Sinko, P. J. The effect of physical barriers and properties on the oral absorption of particulates. *Adv. Drug Delivery Rev.* **1998**, *34* (2–3), 135–154.
- (3) Ponchel, G.; Irache, J. Specific and non-specific bioadhesive particulate systems for oral delivery to the gastrointestinal tract. *Adv. Drug Delivery Rev.* **1998**, *34*, 191–219.

- (4) Mahdavi, A.; et al. A biodegradable and biocompatible gecko-inspired tissue adhesive. *Proc. Nat. Acad. Sci. U.S.A.* **2008**, *105*, 2307–12.
- (5) Lee, H.; Lee, B. P.; Messersmith, P. B. A reversible wet/dry adhesive inspired by mussels and geckos. *Nature* **2007**, *448*, 338–41.
- (6) Sudhakar, Y.; Kuotsu, K.; Bandyopadhyay, A. K. Buccal bioadhesive drug delivery - A promising option for orally less efficient drugs. *J. Controlled Release* **2006**, *114*, 15–40.
- (7) Smart, J. D. The basics and underlying mechanisms of mucoadhesion. *Adv. Drug Delivery Rev.* **2005**, *57*, 1556–1568.
- (8) Khanvilkar, K.; Donovan, M. D.; Flanagan, D. R. Drug transfer through mucus. *Adv. Drug Delivery Rev.* **2001**, *48*, 173–193.
- (9) Naisbett, B.; Woodley, J. The Potential Use Of Tomato Lectin For Oral-Drug Delivery.3. Bioadhesion In-Vivo. *Int. J. Pharm.* **1995**, *114*, 227–236.
- (10) Bies, C.; Lehr, C.-M.; Woodley, J. F. Lectin-mediated drug targeting: history and applications. *Adv. Drug Delivery Rev.* **2004**, *56*, 425.
- (11) Lehr, C. M.; et al. An estimate of turnover time of intestinal mucus gel layer in the rat in situ loop. *Int. J. Pharm.* **1991**, *70*, 235–240.
- (12) Cheng, H.; Bjerknes, M. Cell production in mouse intestinal epithelium measured by stathmokinetic flow cytometry and coulter particle counting. *Anat. Rec.* **1995**, *207*, 427–434.
- (13) Sun, W.; Neuzil, P.; Kustandi, T. S.; Oh, S.; Samper, V. D. The nature of the gecko lizard adhesive force. *Biophys. J.* **2005**, *89*, L14–7.
- (14) Autumn, K.; et al. Evidence for van der Waals adhesion in gecko setae. *Proc. Nat. Acad. Sci. U.S.A.* **2002**, *99*, 12252–12256.
- (15) Autumn, K.; et al. Adhesive force of a single gecko foot-hair. *Nature* **2000**, *405*, 681–685.
- (16) Huber, G.; et al. Evidence for capillarity contributions to gecko adhesion from single spatula nanomechanical measurements. *Proc. Nat. Acad. Sci. U.S.A.* **2005**, *102*, 16293–6.
- (17) Autumn, K.; Dittmore, A.; Santos, D.; Spenko, M.; Cutkosky, M. Frictional adhesion: a new angle on gecko attachment. *J. Exp. Biol.* **2006**, *209* (18), 3569–3579.
- (18) Huber, G.; et al. Resolving the nanoscale adhesion of individual gecko spatula by atomic force microscopy. *Biol. Lett.* **2005**, *1* (1), 2–4.
- (19) Lee, J.; Majidi, C.; Schubert, B.; Fearing, R. S. Sliding induced adhesion of stiff polymer microfiber arrays: I. Macroscale behavior. *J. R. Soc. Interface* **2008**, *5*, 835–844.
- (20) Kim, S.; Sitti, M. Biologically inspired polymer microfibers with spatulate tips as repeatable fibrillar adhesives. *Appl. Phys. Lett.* **2006**, *89* (26), 26911–13.
- (21) Yurdumakan, B.; Raravikar, N. R.; Ajayan, P. M.; Dhinojwala, A. Synthetic gecko foot-hairs from multiwalled carbon nanotubes. *Chem. Commun.*, **2005**, 3799–3801.
- (22) del Campo, A.; Arzt, E. Design parameters and current fabrication approaches for developing bioinspired dry adhesives. *Macromo. Biosci.* **2007**, *7*, 118–127.
- (23) Peressadko, A.; Gorb, S. N. When less is more: Experimental evidence for tenacity enhancement by division of contact area. *J. Adhes.* **2004**, *80* (4), 247–261.
- (24) Spolenak, R.; Gorb, S.; Arzt, E. Adhesion design maps for bio-inspired attachment systems. *Acta Biomater.* **2005**, *1*, 5–13.
- (25) Spolenak, R.; Gorb, S.; Gao, H. J.; Arzt, E. Effects of contact shape on the scaling of biological attachments. *Proc. R. Soc. London, Ser. A.* **2005**, *461* (2054), 305–319.
- (26) Mygind, N.; Dahl, R. Anatomy, physiology, and function of the nasal cavities in health and disease. *Adv. Drug Delivery Rev.* **1998**, *29*, 3–12.
- (27) Alberts, B.; Johnson, A.; Lewis, J.; Raff, M.; Roberts, K.; Walter, P. *Molecular Biology of the Cell*, 4th ed.; Garland Science: New York, 2002; Chapter 16.
- (28) Tortora, G. J.; Anagnostakos, N. P. *Principles of Anatomy and Physiology*; Canfield Press: San Francisco, 1975; p 44.
- (29) DeSesso, J. M.; Williams, A. L. Chapter 21 Contrasting the Gastrointestinal Tracts of Mammals: Factors that Influence Absorption. *Annu. Rep. Med. Chem.* **2008**, *43*, 353–371.
- (30) Cui, Y.; Lauhon, L. J.; Gudixsen, M. S.; Wang, J. F.; Lieber, C. M. Diameter-controlled synthesis of single-crystal silicon nanowires. *Appl. Phys. Lett.* **2001**, *78*, 2214–2216.
- (31) Pinto, M.; Robineleon, S.; Appay, M. D.; Kedingler, M.; Triadou, N.; Dussaulx, E.; Lacroix, B.; Simonassmann, P.; Haffen, K.; Fogh, J.; Zweibaum, A. Enterocyte-Like Differentiation and Polarization of the Human-Colon Carcinoma Cell-Line Caco-2 in Culture. *Biol. Cell* **1983**, *47* (3), 323–330.
- (32) Lehr, C. M.; et al. Bioadhesion By Means Of Specific Binding Of Tomato Lectin. *Pharm. Res.* **1992**, *9*, 547–553.
- (33) Gabor, F.; Wirth, M. Lectin-mediated drug delivery: fundamentals and perspectives. *STP Pharma. Sci.* **2003**, *13* (1), 3–16.
- (34) Kilpatrick, D. C.; Pusztai, A.; Grant, G.; Graham, C.; Ewen, S. W. B. Tomato Lectin Resists Digestion In The Mammalian Alimentary Canal And Binds To Intestinal Villi Without Deleterious Effects. *FEBS Lett.* **1985**, *185* (2), 299–305.
- (35) Nel, A.; Xia, T.; Madler, L.; Li, N. Toxic potential of materials at the nanolevel. *Science* **2006**, *311*, 622–627.
- (36) Ainslie, K. M.; Tao, S. L.; Popat, K. C.; Daniels, H.; Hardev, V.; Grimes, C. A.; Desai, T. A. In vitro inflammatory response of nanostructured titania, silicon oxide, and polycaprolactone. *J. Biomed. Mater. Res. A* **2008**. Published Online: 5 Nov 2008.
- (37) Schurr, M. O.; Schostek, S.; Ho, C.; Rieber, F.; Menciassi, A. Microtechnologies in medicine: An overview. *Minimally Invasive Ther.* **2007**, *16* (2), 76–86.
- (38) Staples, M.; Daniel, K.; Cima, M. J.; Langer, R. Application of Micro- and Nano-Electromechanical Devices to Drug Delivery. *Pharm. Res.* **2006**, *23* (5), 847–863.
- (39) Duan, X. F.; Lieber, C. M. General synthesis of compound semiconductor nanowires. *Adv. Mater.* **2000**, *12*, 298–302.
- (40) Sultzbaugh, K. J.; Speaker, T. J. A method to attach lectins to the surface of spermine alginate microcapsules based on the avidin biotin interaction. *J. Microencapsulation* **1996**, *13*, 363–376.
- (41) Butt, H. J.; Jaschke, M. Calculation Of Thermal Noise In Atomic-Force Microscopy. *Nanotechnology* **1995**, *6*, 1–7.
- (42) Hutter, J. L.; Bechhoefer, J. Calibration Of Atomic-Force Microscope Tips. *Rev. Sci. Instrum.* **1993**, *64*, 1868–1873.
- (43) Salapaka, M. V.; Bergh, H. S.; Lai, J.; Majumdar, A.; McFarland, E. Multi-mode noise analysis of cantilevers for scanning probe microscopy. *J. App. Phys.* **1997**, *81* (6), 2480–2487.
- (44) Kappl, M.; Butt, H. J. The colloidal probe technique and its application to adhesion force measurements. *Part. Part. Syst. Character.* **2002**, *19*, 129–143.
- (45) Sader, J. E.; Larson, I.; Mulvaney, P.; White, L. R. Method For The Calibration Of Atomic-Force Microscope Cantilevers. *Rev. Sci. Instrum.* **1995**, *66*, 3789–3798.
- (46) Cleveland, J. P.; Manne, S.; Bocek, D.; Hansma, P. K. A Nondestructive Method For Determining The Spring Constant Of Cantilevers For Scanning Force Microscopy. *Rev. Sci. Instrum.* **1993**, *64*, 403–405.
- (47) Proksch, R.; Schaffer, T. E.; Cleveland, J. P.; Callahan, R. C.; Viani, M. B. Finite optical spot size and position corrections in thermal spring constant calibration. *Nanotechnology* **2004**, *15*, 1344–1350.
- (48) Jensen, K.; Mickelson, W.; Kis, A.; Zettl, A. Buckling and kinking force measurements on individual multiwalled carbon nanotubes. *Phys. Rev. B: Condens. Matter* **2007**, *76*.
- (49) Timoshenko, S., Gere, J. *Theory of Elastic Stability*; McGraw-Hill: New York, 1961.
- (50) Obataya, I.; Nakamura, C.; Han, S.; Nakamura, N.; Miyake, J. Nanoscale operation of a living cell using an atomic force microscope with a nanoneedle. *Nano Lett.* **2005**, *5*, 27–30.
- (51) Vakarelski, I. U.; Brown, S. C.; Higashitani, K.; Moudgil, B. M. Penetration of living cell membranes with fortified carbon nanotube tips. *Langmuir* **2007**, *23*, 10893–10896.

NL803219F